PERGAMON

Journal of Structural Geology 23 (2001) 407–419

JOURNAL OF STRUCTURAL GEOLOGY

www.elsevier.nl/locate/jstrugeo

Contemporary in situ stress determinations at three sites in Scotland and northern England

Arnfried Becker[a], Colin A. Davenport[b,*]

[a]*Institut für Geophysik, ETH Zürich, CH-8093 Zürich, Switzerland*
[b]*School of Environmental Sciences, University of East Anglia, Norwich NR4 7TJ, UK*

Received 19 January 2000; accepted 17 July 2000

Abstract

During 1987, in situ stress measurements using two overcoring techniques (doorstopper and triaxial strain cell) were made in England and Scotland as part of the former SFB 108 Project 'Stress and Stress Release in the Lithosphere' at Karlsruhe University. The results for three of the test sites—Spittal in Caithness, Gartur in the Midland Valley of Scotland and at Burton in Cumbria—are reported. Complementary studies on cores from Gartur using portable ASR equipment are included. The maximum horizontal stress orientations agree closely with those seen in the general contemporary stress field in NW Europe. These results confirm that, in favourable circumstances, these shallow methods offer effective approaches to the acquisition of reliable contemporary stress information, whether derived from boreholes or rock cores.

1. Introduction

In a discussion at the Royal Society meeting 'Tectonic Stress in the Lithosphere' held on 10 and 11 April 1991, Paul Hancock reported "… some unpublished overcoring measurements. The first set were made in the central valley of Scotland and the second set were made in the middle of the Orcadian Plateau in Caithness…" (Whitmarsh et al., 1991, p. 178). These measurements are those which were carried out with Paul's guidance in 1987 during post-doctoral studies at the Department of Geology of Bristol University by one of the authors (A.B.). In two extended field reconnaissances across England and Scotland, four test sites were selected for in situ stress measurements using two different overcoring techniques, i.e. the doorstopper and the triaxial strain cell methods. The drilling and in situ measurements were made using the equipment of the former SFB 108 Project 'Stress and Stress Release in the Lithosphere', based at Karlsruhe University. In the meantime, the results of these stress measurements have been published (Becker and Paladini, 1990, 1992; Davenport et al., 1989), and have also been included in the data base of the 'World Stress Map'. However, apart from the test site in southern England (Becker et al., 1990), the details of the results from the remaining three sites have not been published. To complete these studies which, at various times, involved Paul and the authors, the results from the sites in northern England and Scotland are presented in this publication as a personal tribute to Paul as a colleague and friend. The locations of the test sites are given in Fig. 1, which are Spittal in Caithness, Gartur in the Midland Valley of Scotland and the site in England at Burton in Cumbria. All these sites are located in flat-lying sedimentary rocks in low topography surroundings, as illustrated in Fig. 2.

2. Spittal test site

2.1. Topography and geological setting

The test site (3° 25′ 31″ W, 58° 28′ 10″ N) is located in the quarry immediately north of Spittal, a small village in the centre of Caithness, northeastern most Scotland (Fig. 1), in an area of low topographic ridges and flat, poorly drained hollows (flows) at the centre of the Orcadian Plateau (Fig. 3). The quarry has been excavated into almost flat ground at an elevation of circa 120 m a.S.L., from where the ground rises gently northward to the summit of Spittal Hill (176 m a.S.L.) (Fig. 2a). Thin deposits of boulder clay and similar glacial deposits mantle the bedrock of the area. The horizontally bedded pale grey calcareous mudstones and siltstones of the Spittal (Latheron) subgroup of the Upper Caithness Flagstone Group of Middle Devonian age form

* Corresponding author. Fax: +44-(0)1603-592-949.
E-mail address: c.davenport@uea.ac.uk (C.A. Davenport).

0191-8141/01/$ - see front matter
PII: S0191-8141(00)00123-1

Fig. 1. Location of in situ stress measuring test sites in mainland Britain.

near horizontal planar benches in these quarries. These rocks were deposited in the Devonian Old Red Sandstone (ORS) Caithness–Orkney Lake, along with finely laminated and fissile 'flagstones' which were quarried extensively for roofing slate in the past (British Geological Survey, 1985). The quarry at Spittal provides opportunities to investigate the properties of widely jointed rock layers (Fig. 2b), which have remained virtually undeformed since Devonian times. Bedding plane dips rarely exceed 3°, the result of gentle folding along N–S-trending axes, the nearest of which is more than 4 km to the east. Although the rocks are essentially unfaulted, small-scale low angle thrust faults are developed locally throughout the area and there is occasional local evidence of bedding-parallel movement. These local bedding-plane slips have been reported to be ice-movement effects. They are seen also at Spittal, which is far from a significant fault (5 km) and where fold flexure effects would not be expected.

2.2. Triaxial strain cell method

Most of the triaxial strain cells presently used for in situ stress determinations in rock are modifications of the measuring tool originally introduced by Leeman and Hayes (1966) for 3-D stress determination in single boreholes. Such a modification is the CSIR triaxial strain cell from Interfels (Bad Bentheim), which has the advantage of allowing stress measurements below the ground water table. The CSIR triaxial strain cell method is a typical representative of overcoring relief techniques, where strain gauges are used to measure strains caused by overcoring-induced stress relief. The sequence required for the triaxial strain cell overcoring technique is shown in Fig. 4. A borehole with a diameter of 116 mm is drilled into the rock to a point where the stress is to be measured (a); a pilot hole about 1 m long and 37 mm in diameter is then drilled from the bottom of and concentric with the main borehole (b); after inspection of the drill core and cleaning of the pilot borehole (c), the triaxial strain cell, which is attached to the installing tool, is inserted into the pilot hole. After orientation of the strain cell, three strain gauge rosettes with four strain gauges each, mounted in 0–120–240° directions, are forced outwards against the sidewall of the pilot hole, glued into position and the first strain readings are taken (d). After the glue has set, which needs several hours, the final strain readings are taken and the installing tool is removed (e). Now the triaxial strain cell is overcored, again using the 116-mm-diameter core bit, which has already been used to drill the main borehole (f). The core with the glued-in triaxial strain cell is broken off at the bottom of the borehole (g). After recovery of the core, the triaxial strain cell is again plugged into the installing tool, so that the strains caused by stress relief can be measured (h).

The calculation of stresses from measured strains on the wall of a borehole is based primarily on the conversion of secondary stresses on the borehole wall into the primary far-field stresses following the theory given by Hiramatsu and Oka (1962). Because the stress state on the borehole wall is 2-D, i.e. all radial stress components of the stress tensor are zero, strains can be converted easily into stresses using Hooke's law of linear elasticity. In addition, the conversion of measured strains in certain directions into the components of the strain tensor is based on standard procedures (cf. Jaeger and Cook, 1979, p. 51). Transverse anisotropy can be taken into account for the Caithness Flagstones by assuming different elastic behaviour under loads parallel and perpendicular to the bedding plane. Since the z-axis of the Cartesian coordinate system is vertical and parallel to the borehole long axis with a positive direction towards the borehole mouth, then if the x-axis is north, the y-axis is west. The gauges of the strain gauge rosettes are oriented horizontally (0°), inclined (45°), vertically (90°) and inclined (135°) anticlockwise. Because there are four strain gauges in each rosette and the rosettes of the CSIR triaxial strain cell, type Interfels, are oriented in a Y configuration (0–120–240°), 12 equations can be used to convert the individually measured strains of the single strain gauges (e_1–e_{12}) into far-field stresses (in Cartesian coordinates):

$\underline{\varphi = 0° = 180°}$

$$\theta = 0°: \quad e_1 = C_3\sigma_x + C_1\sigma_y + C_2\sigma_z \tag{1}$$

$$45°: \quad e_2 = C_7\sigma_x + C_5\sigma_y + C_6\sigma_z + 4C_8\tau_{yz} \tag{2}$$

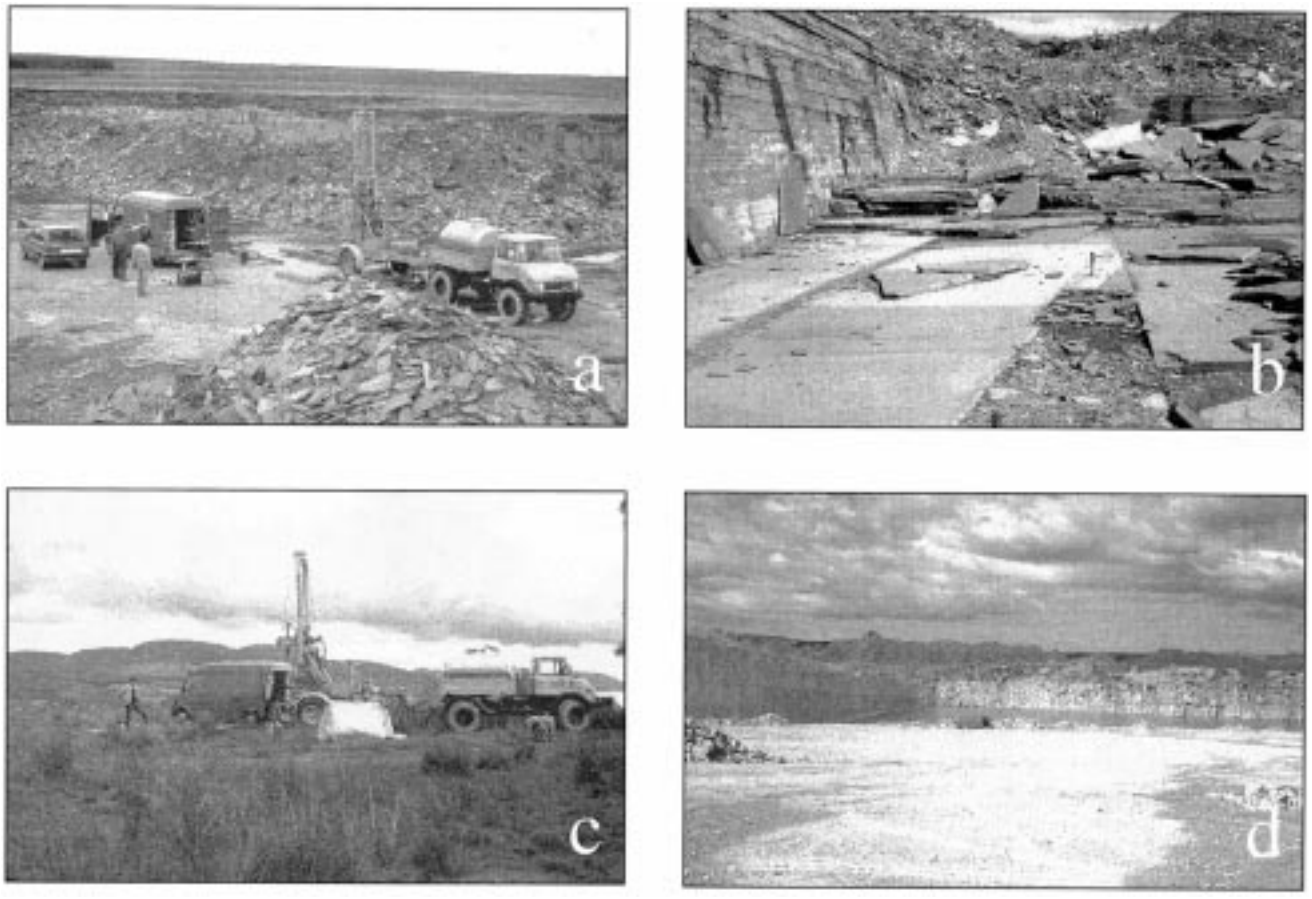

Fig. 2. Site situations. (a) Spittal quarry with view to the north in the direction of Spittal Hill. Equipment from right to left: truck with a 2-m^3 water tank, a drilling rig immediately behind the truck and workshop van, before which is a triaxial strain cell in preparation. (b) Thinly bedded and laminated widely spaced jointed siltstones of the Spittal Beds in Spittal quarry. (c) Gartur site, northern Midland Valley, looking northwards towards the Menteith Hills, showing the drilling equipment. (d) Burton site showing Holme Park quarry limestone exposures.

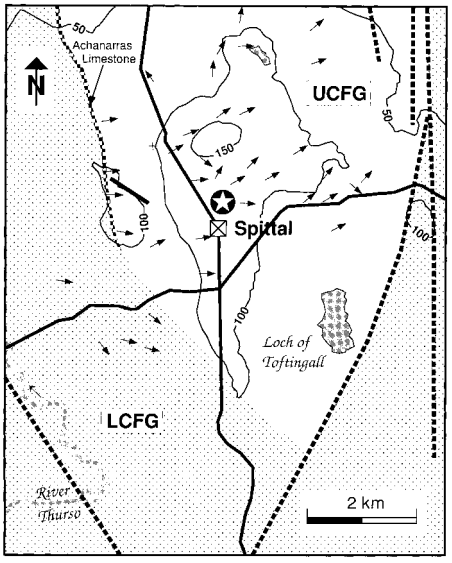

Fig. 3. Triaxial strain cell test site north of Spittal (star in black circle). Height contours are given in metres a.S.L. Bold solid or hatched lines indicate proven or assumed faults, UCFG and LCFG denote Upper and Lower Caithness Flagstone Group, respectively. Arrows indicate dip directions of layering, which is less than or equal to 5° for the dip directions shown.

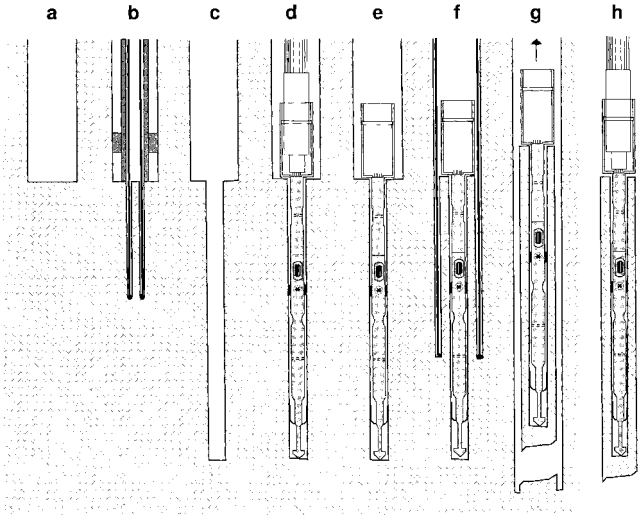

Fig. 4. Stages of the triaxial strain cell overcoring technique.

$$90°: \quad e_3 = C_2\sigma_x + C_2\sigma_y + C_4\sigma_z \tag{3}$$

$$135°: \quad e_4 = C_7\sigma_x + C_5\sigma_y + C_6\sigma_z - 4C_8\tau_{yz} \tag{4}$$

$\underline{\varphi = 60° = 240°}$

$$\theta = 0°: \quad e_5 = \frac{1}{4}(3C_1 + C_3)\sigma_x + \frac{1}{4}(C_1 + 3C_3)\sigma_y + C_2\sigma_z + \frac{\sqrt{3}}{2}(C_3 - C_1)\tau_{xy} \tag{5}$$

$$45°: \quad e_6 = \frac{1}{4}(3C_5 + C_7)\sigma_x + \frac{1}{4}(C_5 + 3C_7)\sigma_y + C_6\sigma_z + \frac{\sqrt{3}}{2}(C_7 - C_5)\tau_{xy} + 2\sqrt{3}C_8\tau_{xz} - 2C_8\tau_{yz} \tag{6}$$

$$90°: \quad e_7 = C_2\sigma_x + C_2\sigma_y + C_4\sigma_z \tag{7}$$

$$135°: \quad e_8 = \frac{1}{4}(3C_5 + C_7)\sigma_x + \frac{1}{4}(C_5 + 3C_7)\sigma_y + C_6\sigma_z + \frac{\sqrt{3}}{2}(C_7 - C_5)\tau_{xy} - 2\sqrt{3}C_8\tau_{xz} + 2C_8\tau_{yz} \tag{8}$$

$\underline{\varphi = 120° = 300°}$

$$\theta = 0°: \quad e_9 = \frac{1}{4}(3C_1 + C_3)\sigma_x + \frac{1}{4}(C_1 + 3C_3)\sigma_y + C_2\sigma_z + \frac{\sqrt{3}}{2}(C_1 - C_3)\tau_{xy} \tag{9}$$

$$45°: \quad e_{10} = \frac{1}{4}(3C_5 + C_7)\sigma_x + \frac{1}{4}(C_5 + 3C_7)\sigma_y + C_6\sigma_z + \frac{\sqrt{3}}{2}(C_5 - C_7)\tau_{xy} - 2\sqrt{3}C_8\tau_{xz} - 2C_8\tau_{yz} \tag{10}$$

$$90°: \quad e_{11} = C_2\sigma_x + C_2\sigma_y + C_4\sigma_z \tag{11}$$

$$135°: \quad e_{12} = \frac{1}{4}(3C_5 + C_7)\sigma_x + \frac{1}{4}(C_5 + 3C_7)\sigma_y + C_6\sigma_z + \frac{\sqrt{3}}{2}(C_5 - C_7)\tau_{xy} + 2\sqrt{3}C_8\tau_{xz} + 2C_8\tau_{yz}. \tag{12}$$

The constants C_1–C_8 are defined as follows:

$$C_1 = \frac{1}{E_1}\left(3 - 2\nu_2^2\frac{E_1}{E_2}\right)$$

$$C_2 = -\frac{\nu_2}{E_2}$$

$$C_3 = -\frac{1}{E_1}\left(1 - 2\nu_2^2\frac{E_1}{E_2}\right)$$

$$C_4 = \frac{1}{E_2}$$

$$C_5 = \frac{1}{2}\left(\frac{3}{E_1} - \frac{\nu_2}{E_2} - \frac{2\nu_2^2}{E_2}\right)$$

$$C_6 = \frac{1}{2}\left(\frac{1}{E_2} - \frac{\nu_2}{E_2}\right)$$

$$C_7 = -\frac{1}{2}\left(\frac{1}{E_1} + \frac{\nu_2}{E_2} - \frac{2\nu_2^2}{E_2}\right)$$

$$C_8 = \frac{1}{4G_2}.$$

The elastic parameters, Young's modulus E_1 and Poisson's ratio ν_1, are those for load in the plane of isotropy (i.e. parallel to bedding), and E_2 and ν_2 are those for load perpendicular to the plane of isotropy. The shear modulus G_2 can be determined after Amadei (1983):

$$G_2 = \frac{E_3}{2(1 + \nu_3)}. \tag{13}$$

In this case, the elastic parameters E_3 and ν_3 are those for a load applied at 45° to the plane of isotropy. Alternatively, the shear modulus can be estimated using only Young's moduli E_1 and E_2 and Poisson's ratio ν_2 (Lekhnitskii, 1963):

$$G_2 = \frac{E_1}{1 + \frac{E_1}{E_2}(1 + 2\nu_2)}. \tag{14}$$

In the case of isotropic linear-elastic behaviour, $E_1 = E_2 = E_3 = E$, $\nu_1 = \nu_2 = \nu_3 = \nu$ and $G_2 = G$.

2.3. Determination of elastic parameters

The Young's modulus was determined in the laboratory by uniaxial loading at a rate of 6.25 MPa/min on nine core samples with a diameter of 67 mm and a length/width ratio of approximately 2:1, the length of the core samples varying between 125.8 and 140.0 mm. Additionally, in situ determinations were carried out in boreholes using the Goodman Jack. Poisson's ratios were determined only in the uniaxial loading tests.

The uniaxial loading tests showed linear-elastic or very close linear-elastic load–deformation relationships, with only a very weak hysteresis in samples taken parallel and perpendicular to the plane of isotropy. However, a more

Table 1
Results of Young's modulus and Poisson's ratio determinations from uniaxial loading tests on core samples and density values for Spittal[a]

E_1 (MPa)	ν_1 (—)	ρ (kg/m^3)	E_2 (MPa)	ν_2 (—)	ρ (kg/m^3)	E_3 (MPa)	ν_3 (—)	ρ (kg/m^3)
58880	0.23	2650	44430	0.24	2670	46570	0.18	2690
58300	0.24	2670	42930	0.27	2690	43980	0.18	2660
57160	0.23	2680	43400	0.26	2680	43520	0.18	2650

[a] The elastic parameters E_1 and ν_1 are those for load parallel, E_2 and ν_2 those for load perpendicular, and E_3 and ν_3 those for load oblique to the plane of isotropy (bedding).

pronounced hysteresis and non-linearity developed in the case of the samples taken oblique to the bedding plane. Also, the uniaxial compressional strength shows clear differences between the samples taken parallel and vertical to the bedding plane and those taken obliquely (45°), i.e. in the first two cases, with the exception of one (143), all lie between 200 and 230 MPa, and in the third case between 100 and 120 MPa.

The results of the Young's modulus and Poisson's ratio determinations from the uniaxial loading tests are shown in Table 1. The highest values of Young's modulus are those parallel to bedding and lowest perpendicular to bedding. The Poisson's ratios ν_1 and ν_2 are similar, with ν_3 significantly lower. As indicate by the E_1/E_2 ratio of 1.3, the anisotropy in the Spittal beds is only weakly developed.

In addition to the laboratory uniaxial loading tests, new boreholes drilled at 76 mm diameter parallel to the bedding plane permitted in situ Goodman Jack tests parallel, oblique (45°) and vertical to the bedding plane. The secant modulus for the third loading cycle (in some cases also for the second) was calculated, using as the lower limit a load of 5 MPa and as the upper limit the maximum load of the considered loading cycle. The revised equation given by Heuze and Amadei (1985) is used for the Young's modulus calculation:

$$E = 0.86{\cdot}0.93D\frac{\Delta Q_h}{\Delta D}T^*, \tag{15}$$

where D is the diameter of the borehole, ΔD the change in diameter, ΔQ_h the line pressure change and T^* a constant which has values between 1.474 and 1.397 for Poisson's ratios between 0.2 and 0.3. The results are given in Table 2. For the Goodman Jack measurements, the anisotropy ratio is slightly higher than for the uniaxial loading tests, i.e. $E_1/E_2 = 1.7$. This may reflect the different kind of loading in the two tests, i.e. in a uniaxial loading test perpendicular to the bedding planes are under compression, whereas in a Goodman Jack test the load is oriented such that the bedding planes could be forced apart. Most of these bedding planes are fissile and were used in the quarrying of the flagstones by splitting the rock into thin slabs. This fissility would be expected to reduce the tensile strength parallel with the bedding planes, which would explain the fact that the Goodman Jack Young's modulus perpendicular to the bedding plane (E_2) is slightly lower, thus supplying a slight overestimate of the E_1/E_2 ratio.

Table 2
Results of Young's modulus determinations from Goodman Jack tests in situ for Spittal[a]

E_{G1} (MPa)	E_{G2} (MPa)	E_{G3} (MPa)
12390	5210	9120
9500	7560	10370
11090	4350	5260
10250	6960	7350
8400		
11040		

[a] The elastic parameter E_1 is that for load parallel, E_2 that for load perpendicular and E_3 that for load oblique to the plane of isotropy (bedding).

The shear modulus (G_2) determination using the Lekhnitskii (1963) method (Eq. (14)) is based on elastic parameters determined parallel and perpendicular to the bedding plane. For this site, this equation gives $G_2 = 19{,}200$ MPa. The alternative approach of Amadei (1983) (Eq. (13)) is based on elastic parameters determined at 45° to the bedding plane, giving a value of $G_2 = 18{,}900$ MPa. Both approaches give similar values, but, from a practical point of view, Lekhnitskii's approach has the advantage that, for G_2 determination, only elastic parameters are used which are needed elsewhere for stress calculations. When the Young's modulus determinations using the Goodman Jack results are applied in the two approaches, more significant discrepancies are revealed, i.e. $G_2 = 3400$ MPa (Amadei, 1983) or $G_2 = 2900$ MPa (Lekhnitskii, 1963). As mentioned above, this is to be expected because of the higher E_1/E_2 ratio caused by the reduced Young's modulus perpendicular to the fissile bedding.

2.4. Results of triaxial strain cell measurements

Eight triaxial strain cell tests (Spittal I–VIII) were carried out in one borehole at a depth of between 9.30 and 27.30 m. In the tests Spittal I and IV, one of the strain gauge rosettes failed, probably due to sand grains on the borehole wall that destroyed the strain gauges. Also, Spittal II supplied anomalous results with respect to the principal axis orientations and the magnitudes, so that this measurement is considered to have failed. The remaining five results are shown in Table 3. The principal axis orientations are corrected for the difference between magnetic north and

Table 3
Results of five triaxial strain cell measurements in Spittal quarry[a]

Test	Isotropic elasticity			Anisotropic elasticity		Principal stresses
	Dip direction/dip	Magnitude (MPa)	Magnitude (MPa)	Dip direction/dip	Magnitude (MPa)	
Spittal III	309/60	15.7	3.4	313/44	15.9	σ_1
	155/27	10.5	2.2	167/41	11.7	σ_2
	59/11	8.3	1.8	61/18	9.6	σ_3
Spittal V	349/83	28.4	6.1	348/83	25.6	σ_1
	98/02	6.8	1.5	98/02	7.7	σ_2
	188/06	2.6	0.6	188/07	2.8	σ_3
Spittal VI	162/80	17.2	3.7	162/79	15.6	σ_1
	309/08	2.9	0.6	311/10	3.2	σ_2
	40/05	2.4	0.5	42/06	2.6	σ_3
Spittal VII	64/82	8.4	1.8	76/75	7.9	σ_1
	305/04	5.8	1.2	307/09	6.8	σ_2
	214/07	4.8	1.0	215/11	5.6	σ_3
Spittal VIII	83/79	13.9	3.0	85/76	12.8	σ_1
	271/11	6.2	1.3	272/14	7.2	σ_2
	182/02	2.4	0.5	181/02	2.7	σ_3

[a] The stress magnitudes for isotropic elastic behaviour are calculated for E and E_G using values of 48,800 and 10,450 MPa, respectively, and $\nu = 0.22$. The stress magnitudes for transversely anisotropic elastic behaviour are calculated using Young's modulus and Poisson's ratio values derived from Table 1.

true north, which in 1987 was about 8°W. To see the difference between transversal anisotropic and isotropic stress calculations, both results are presented in Table 3. In isotropic calculations, an average Young's modulus of $E = 48.8$ GPa and a Poisson's ratio $\nu = 0.22$ were derived, and for anisotropic calculations $E_1 = 58.1$ GPa, $E_2 = 43.6$ GPa, $E_3 = 44.7$ GPa and $\nu_1 = 0.23$, $\nu_2 = 0.26$ and $\nu_3 = 0.18$. With the exception of Spittal III, all σ_1 axes are close to vertical, the remaining two principal axes close to the horizontal. There is no significant difference between the axis orientations of the two calculations, except for Spittal III, where the principal axes are not (approximately) within or vertical to the plane of isotropy. The three principal axis orientations for the five tests for the case of isotropic calculation are shown in Fig. 5. The small difference between both sets of results is caused by the minor anisotropy ($E_1/E_2 = 1.3$), and the favourable orientation of the principal axes with respect to the plane of isotropy in most cases.

In the case of stress magnitudes, the differences between isotropic and anisotropic calculations are more obvious, best seen in the vertical stress magnitudes listed in Table 3. With an average density for the rocks in Spittal of 2670 kg/m^3, the maximum vertical stress should be in the range of 0.4–0.8 MPa (without considering the effects of pore pressure). Even the calculations using the results of the Goodman Jack tests (only parallel to layering because of the already mentioned difficulties with the tests made perpendicular to bedding) supply excessively high stress magnitudes compared to what one would expect. Using equation (4) in Becker and Werner (1995) and the ε_z and ε_x strain values from the individual measurements in Spittal, the Young's modulus can be estimated to be in the range 1.1–3.2 GPa. High stress values can also indicate the presence of high residual stresses in the rock mass. However, such an explanation is considered to be improbable because residual strain measurements have been made in a small test array in 'flagstones' similar to those in Spittal, indicating the absence of significant residual strains (Becker et al., 1997). This is to be expected from the geological history

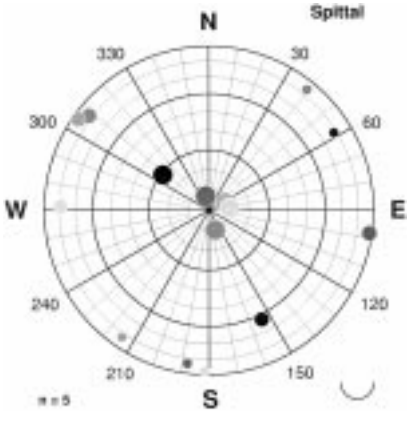

Fig. 5. Orientation of principal axes for individual tests (indicated by spots of different grey scale levels) at Spittal quarry assuming isotropic elasticity: largest = σ_1, smallest = σ_3.

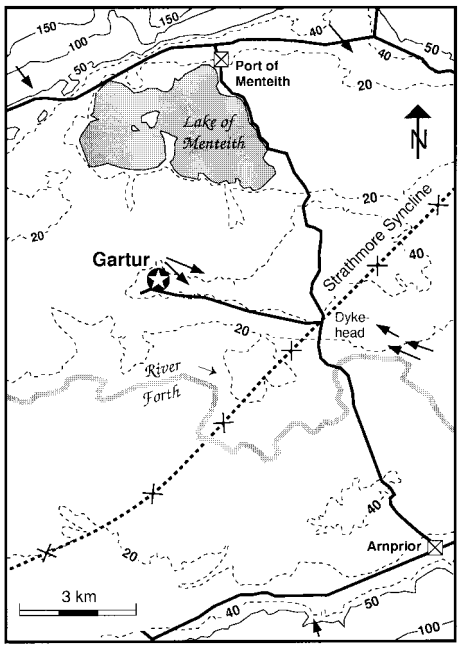

Fig. 6. Triaxial strain cell test site at Gartur (star in black circle). Height contours are given in metres a.S.L. Arrows show bedding dip, rarely exceeding 10°.

of the Spittal beds, which have not suffered strong heating or tectonic deformation. Therefore, it is assumed that the problem of excess stress magnitudes is primarily a problem of the method of determination of the elastic parameters which describe the elastic behaviour of the rock mass.

3. Gartur test site

3.1. Topography and geological setting

At Gartur, the morphology of the Upper Forth Valley has been moulded by the south-eastward extension of the late glaciers of the Loch Lomond Advance (Younger Dryas). Here, the valley has a wide (7 km) floor at an elevation of 20 m a.S.L., containing the meandering channel of the River Forth and the shallow Lake of Menteith (Fig. 6). The terrain rises locally by up to 30 m, for instance at Gartur and on the Menteith Moraine east of Gartur, which marks the limit of the Loch Lomond Advance at circa 10,700 BP (Sissons, 1979). East of this moraine, the bedrock is covered by outwash gravels, which are in turn overlain by marine and estuarine mud-flats. The estuarine deposits of the early post-glacial rise in sea level locally reach a thickness of 100 m above the former shoreline deposits of late-glacial times. The shorelines are tilted to the east as a result of the greater post-glacial uplift in the west. Early Holocene displacements (faults?) have been detected in the vicinity of Arnprior to the southeast of Gartur (Sissons, 1972).

The Devonian Old Red Sandstone (ORS) bedrock is well exposed along the northern edge (showing steep southerly dips) and, along the southern margin (showing less steep northern dips) of this area, within the Forth Valley (Francis et al., 1970). These dip directions are an expression of the late-Caledonian Strathmore Syncline (Fig. 6), which extends from the older Highland border rocks (north of Menteith Hills) to the younger Carboniferous lavas of the southerly Gargunnock Hills. Outcrops are rare in central areas of the valley. The axis of the syncline trends ENE–WSW south of Gartur, where the local dips are not more than a few degrees in the outcropping youngest beds of the Upper Teith Formation (UTF) of the Strathmore Group of the ORS. The UTF comprises light grey sandstones with conglomerates in which true bedding is rare, but shallow cross bedding with dips of up to 12° is common. These rocks are strong well-cemented thickly bedded sandstones with few joints, from which intact 100-mm-diameter cores of up to 1 m length were obtained during stress measurement drilling at the site (Fig. 2c).

3.2. Results of triaxial strain cell measurements

The theoretical considerations for the triaxial strain cell measurements are identical to those for the Spittal site. Because of the homogeneous nature of the core samples, anisotropic elastic rock parameters were not measured. The results of uniaxial loading tests are summarized in Table 4. Compared to Spittal, all the rock parameters are much lower, i.e. Young's modulus is in the range of 22.6 GPa, Poisson's ratio about 0.22, uniaxial loading strength between 76 and 87 MPa, and density around 2400 kg/m^3, all with very low variation. The load–deformation curve shows some non-linearity and a clear hysteresis, so that for the determination of the Young's moduli, the secant modulus of 40–60% of the uniaxial loading strength of the second loading (half) cycle has been used. In addition, Goodman Jack tests in the measuring borehole were carried out using the approach given by Heuze and Amadei (1985). An average value of around 5.7 GPa was obtained from the six results shown in Table 4.

Four triaxial strain cell measurements were carried out in a single borehole at a depth interval of between 13.6 and 19.6 m. The results of the measurements are listed in Table 5. For the calculation of stress magnitudes, the Young's modulus from uniaxial loading tests on core samples and the Goodman Jack Young's modulus have been taken, assuming isotropic (linear) elastic rock behaviour. Gartur

Table 4
Results of rock parameter determinations for Gartur

E (MPa)	ν (—)	ρ (kg/m^3)	E_G (MPa)
22700	0.22	2380	5200
22850	0.21	2380	4770
22350	0.22	2380	4630
		2440	6100
			6240
			7430

Table 5
Results of three triaxial strain cell measurements at Gartur[a]

Test	Dip direction/dip	Magnitude (MPa)	Magnitude (MPa)	Principal stresses	Comment
Gartur I	226/82	5.7	1.5	σ_1	
	131/01	3.2	0.8	σ_2	
	41/08	2.5	0.6	σ_3	
Gartur II	25/87	7.1	1.8	σ_1	
	137/01	3.0	0.8	σ_2	
	227/03	−0.3	−0.1	σ_3	
Gartur III	177/59	2.5	0.6	σ_1	38/60 NW
	18/30	1.6	0.4	σ_2	joint 90 mm
	283/09	0.8	0.2	σ_3	apart
Gartur IV	259/87	6.0	1.5	σ_1	
	126/02	2.4	0.6	σ_2	
	36/02	2.1	0.5	σ_3	

[a] The stress magnitudes for isotropic elastic behaviour are calculated for E and E_G using values of 22,640 and 5730 MPa, respectively, and $\nu = 0.22$.

III is an outlier, due to the fact that one strain gauge rosette has been glued on the borehole wall only 90 mm away from a joint (38/60 NW), which was not recognized before overcoring was finished. The remaining three test results supplied very similar results, with σ_1 almost vertical and σ_2 and σ_3 close to the horizontal (Fig. 7). Again, the same problem arises as already described for Spittal, i.e. the stress magnitudes for the vertical stress component are higher than expected based on the load of the overburden rock mass alone: about 10 times too high when calculated with the Young's modulus from uniaxial loading tests and twice as high when the Goodman Jack Young's modulus is used.

3.3. Anelastic strain recovery

Following in situ stress measurements in 1987, some cores were archived for future laboratory testing. In 1991, Anelastic Strain Recovery (ASR) tests were carried out at the University of East Anglia (UEA) using equipment developed in conjunction with the British Geological Survey (BGS). The ASR rig is a portable system of LVDT strain transducers mounted on carbon fibre rings capable of measuring ASR deformation in cores of up to 100 mm diameter, set in an oil bath for temperature control. The tee-delta rosette is used to provide measurement of strain in four directions, providing a sound basis for the determination of the strain ellipse. The details of the equipment at the various stages of development at BGS and UEA are given in Brereton et al. (1990) and Butterworth (1993). Early results of measurements on Coal Measure (Westphalian) rocks from England were reported in Butterworth et al. (1991). The measurements made on the Gartur core samples were part of an experiment to investigate the potential for using ASR to recover stress data from cores which have been archived in an unconfined state for years. The value of this approach lies in the use of a laboratory method to recover information about in situ stress states from the abundant core material which is gathered for civil engineering and other purposes. This would greatly enhance the data base for certain areas which have not been investigated using in situ techniques. However, archived core would need to meet two requirements, i.e. that the orientation of the core be known (not usually measured in engineering site investigations) and that the lithologies are suitable for 'remembering' the stress state in the ground. The core material from Gartur provided an opportunity to develop this approach, because direct comparison with reliable in situ test data is possible at this site.

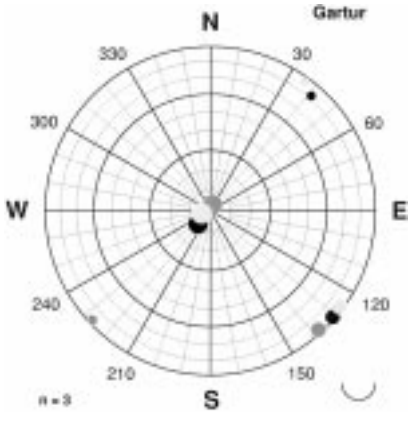

Fig. 7. Orientation of principal axes for individual tests (indicated by spots of different grey scale levels) at Gartur assuming isotropic elasticity: largest = σ_1, smallest = σ_3.

The method of stress recovery involved the undercoring of the archived core (primary core) in the laboratory and rapid placement of the smaller (secondary) core in the ASR rig. A thin-wall core barrel with a diamond-impregnated bit was used to achieve a high quality secondary core with a

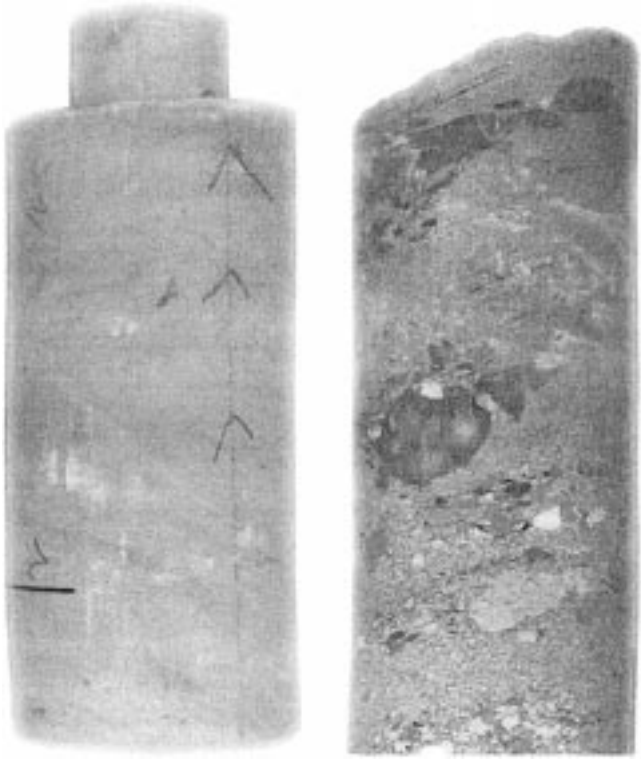

Fig. 8. Old Red Sandstone cores from Gartur used for ASR measurements.

diameter of circa 50 mm and a length of 150 mm. It is assumed that this reduction in diameter has 'removed' most of the rock which has suffered relaxation since primary drilling (Fig. 8). The ends of the core can be trimmed but the secondary core must be at least 150 mm long to accommodate all the ring gauges (Butterworth, 1993).

The test samples from Gartur are well cemented, light grey, strong fine- to medium-grained sandstones with occasional conglomeratic bands (Fig. 8). Initially, core samples were not oriented; however, a bedding fabric which could be matched to that at the site has been used to mark the cores with a scribe line for later orientation of the inferred strain ellipse. The maximum depth of the borehole was 20.2 m and the four samples used in this test came from the lower part of the borehole. The ASR measurement technique is described in detail in Butterworth (1993). The magnitudes of the responses were significantly greater than the system resolution of circa 0.15 μm. Because the principal angle (Φ) is determined with respect to the core orientation line on the sample, these angles can be converted into geographical bearings for direct comparison with those obtained from in situ stress measurements (Table 6). The average difference between the scribe line and the minor strain axis angle is 30°, which converts to a magnetic bearing of 148° for the direction of maximum compression. This is considered to be a good approximation to the maximum horizontal in situ stress orientation average bearing of 131°.

Table 6
Results of ASR measurements on rock cores from Gartur[a]

Sample	Φ ∧ dip (°)	Azimuth
CAD2	45	163
CAD3	25	143
CAD4	30	148

[a] Φ ∧ dip (°) is the angle between the minimum strain axis and the core orientation line for which the azimuth is known.

The close agreement between in situ and ASR maximum horizontal stress orientation shows that the use of ASR to recover stress orientations from archived core is possible. However, more tests need to be done on oriented core from in situ stress sites where suitable lithologies occur.

4. Burton test site

4.1. Topography and geological setting

The site lies about 1 km east of the village of Holme and 2 km north of the village of Burton-in-Kendal, 12 km south of the town of Kendal in Cumbria. The ground to the west of the site is generally flat-lying at 50 m a.S.L., rising from Holme eastwards to Newbiggin Crags by as much as 200 m (Fig. 9). The steep-sided hills of Newbiggin Crags, Holme Park Fell and Clawthorpe Fell have been quarried for limestone, in an area of gently dipping Visean limestones (Fig. 10). These limestones are part of a thick sequence (over 100 m) of carbonate shelf facies units which overlie

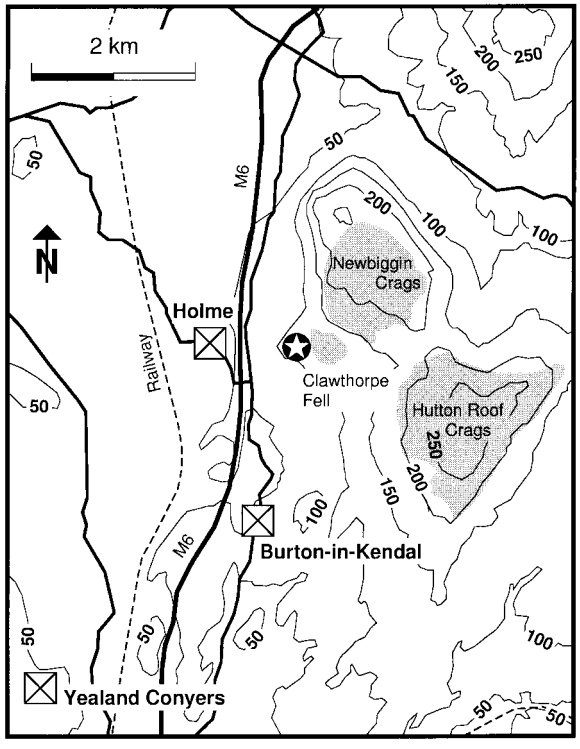

Fig. 9. Doorstopper test site at Burton (star in black circle). Height contours are given in metres a.S.L.

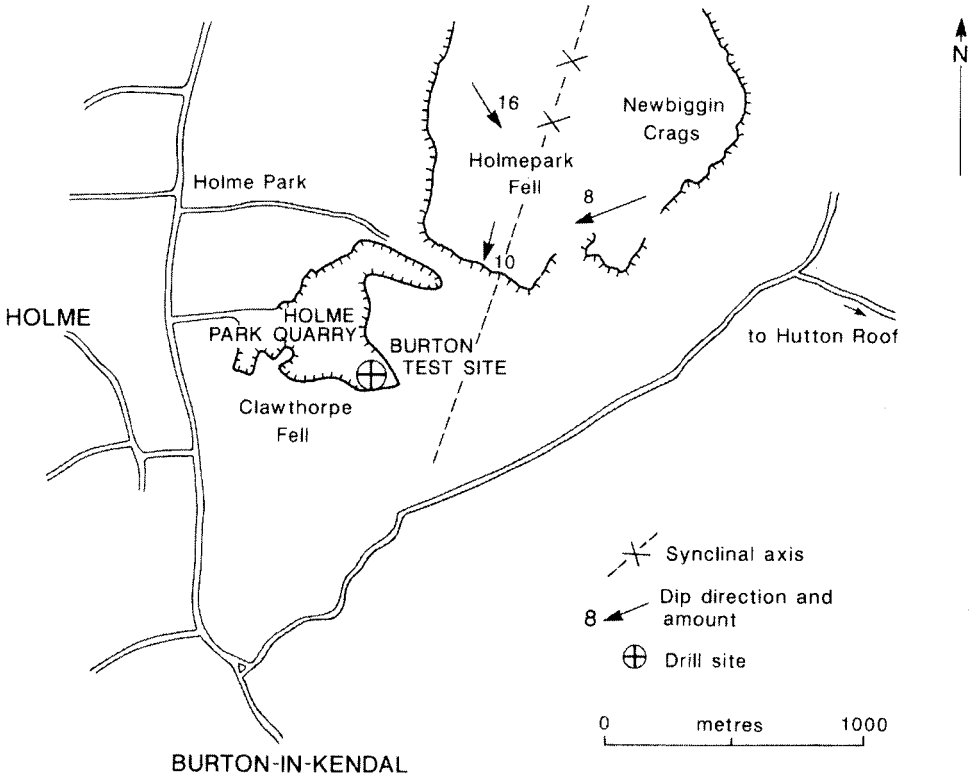

Fig. 10. Structural map of Burton site area. Arrows show dip of bedding.

the metamorphosed Lower Palaeozoic rocks of the English Lake District and the Yorkshire Fells. Many of these units have been recrystallized and dolomitized to become very strong thickly bedded and locally fractured rocks. Jointing and joint-controlled solution weathering at exposed rock surfaces are well developed.

4.2. Doorstopper method

The doorstopper method was developed by Leeman (1964) and is the classical overcoring technique where a strain measuring cell (the so-called doorstopper because of the appearance of the prototype) is glued on the bottom of a borehole and then overcored. In the 1970s and 1980s, the doorstopper and similar strain measuring cells were commonly used in rock mechanics and geodynamics for the determination of in situ stresses. Today, this method is considered to be obsolete and has been replaced, for instance, by the borehole slotter.

The sequence required for the doorstopper overcoring technique is shown in Fig. 11. A borehole with a diameter of 76 mm is drilled into the rock and its bottom is planed, polished and dried (a). An oriented doorstopper is glued to the bottom of the borehole (b). After the glue has set and the initial strain readings for the four strain gauges of the doorstopper are finished, the installing tool is removed (c). The doorstopper is overcored by coring at a diameter of 76 mm (d). The core with the attached doorstopper is broken off at the bottom and removed from the borehole (e). The doorstopper is plugged into the installing tool again (f). As the core is removed from the in situ stress field, strains proportional to stress relief can be measured with the four strain gauges of the doorstopper. The doorstopper cannot be used under water, thus restricting the use of this method to ground above the water table.

No analytical solution that describes the stress state at the bottom of the borehole is available. Therefore, simple Hooke theory for the conversion of strains into stresses is applied, using empirically determined ‘stress concentration factors’ to correct the higher stress magnitudes at the bottom

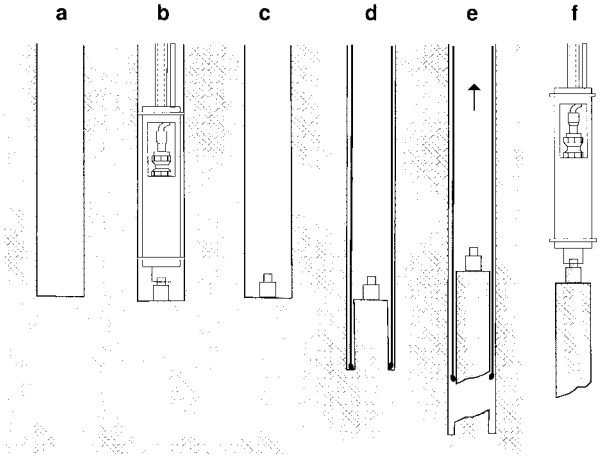

Fig. 11. Stages of the doorstopper overcoring technique.

Table 7
Results of rock parameter determinations for Burton

E (MPa)	ν (—)	ρ (kg/m^3)	E_G (MPa)
72710	0.32	2600	12740
68840	0.30	2600	15650
70790	0.30	2630	18280
		2690	16580
			11640
			12450
			12780
			15700

Table 8
Results of doorstopper measurements for Burton[a]

θ_H	S_H (MPa)	S_h (MPa)	S_H (MPa)	S_h (MPa)
25	5.4	−2.7	1.1	−0.5
1	3.1	−2.1	0.7	−0.4
172	2.1	−0.6	0.5	0.0
156	−0.1	−2.2	0.0	−0.4
0	0.7	−2.0	0.2	−0.4
[172	30.0	8.5	6.2	1.9]
33	7.5	−3.2	1.6	−0.6
40	1.9	−2.2	0.4	−0.4
56	2.6	−4.4	0.6	−0.9
5	12.3	−4.3	2.6	−0.8
[173	53.1	16.6	10.9	3.5]
19	17.0	−3.7	3.5	−0.7
38	0.9	−0.7	0.3	0.0

[a] θ_H is the orientation of maximum horizontal stress S_H.

of the borehole to far-field stress magnitudes (Leeman, 1971).

4.3. Results of doorstopper measurements

In Holme Park quarry near Burton-in-Kendal, 16 doorstopper measurements were carried out in four boreholes at a depth between 2.2 and 6.7 m. Thirteen measurements could be used for the calculation of principal horizontal stresses. The principal axis orientations are corrected for the difference between magnetic north and true north, which in 1987 was about 6°W. The magnitudes of principal horizontal stresses are calculated using the Young's modulus from uniaxial loading tests on four core samples and Goodman Jack tests in situ (Table 7). The results of the doorstopper measurements are listed in Table 8. For the calculation of average horizontal stresses, the results of tests with anomalously high stress magnitudes (in brackets in Table 8) have not been taken into account. The remaining 11 results are given in Fig. 12. The reasons for these anomalously high magnitudes could well be the rapid removal of rock masses by exploitation and local stress concentrations.

5. Discussion

The principal horizontal stresses for individual measurements for the different test sites assuming isotropic elastic behaviour and using the elastic parameters from uniaxial loading tests are shown in Fig. 12, with the average values listed in Table 9. The NW–SE orientations of maximum horizontal stress seen at Gartur and Spittal agree with the general orientation of the tectonic stress field in central and northwestern Europe, corroborating a model of ridge push as the major source of state of tectonic stress in this part of

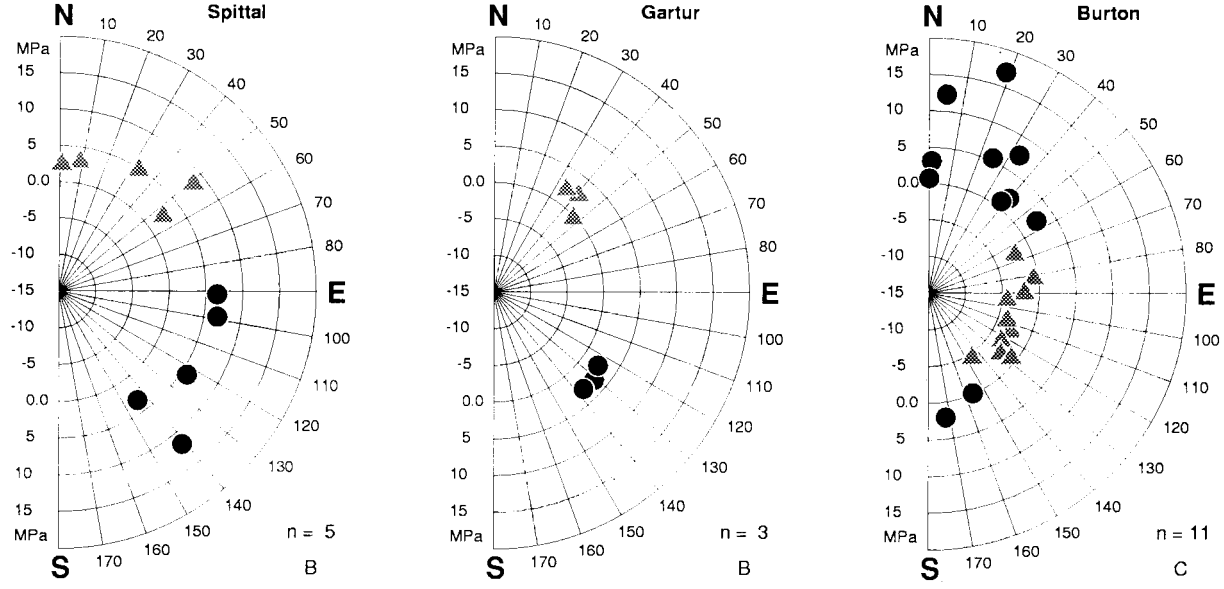

Fig. 12. Principal horizontal in situ stress orientations for individual tests at the three sites. Black circles = S_H, triangles = S_h, calculated assuming isotropic elastic rock behaviour and using the elastic parameters from uniaxial loading tests.

Table 9
Average principal horizontal stress orientations and magnitudes for Spittal, Gartur and Burton calculated using isotropic elastic parameters

Site	θ_H	S_H (MPa)	S_h (MPa)	n
Spittal	120 ± 24	6.8 ± 3.1	4.2 ± 2.6	5
Gartur	131 ± 06	2.9 ± 0.4	1.4 ± 1.5	3
Burton	17 ± 24	4.9 ± 5.4	− 2.6 ± 1.3	11

Europe. Moreover, at Gartur, the laboratory ASR-derived orientations also confirm this dominant direction. However, the test site at Burton shows an NNE–SSW orientation of maximum horizontal stress, which does not fit the general trend. Such exceptions are not so rare in northwestern and central Europe, and have either local causes or are related to regional stress orientations along major crustal structures, for instance in Denmark along the Tornquist line or along the grabens of the central North Sea basin (Müller et al., 1997). Also, around the Irish Sea, in situ stress measurements and also breakout analyses show some anomalies with respect to the orientation of maximum horizontal stress. An interesting observation is described by Brereton and Müller (1991) regarding principal stress orientations across the boundaries of major lithological units in southwestern central England, i.e. an NNW–SSE orientation of S_H in the Carboniferous and a more WNW–ESE orientation in Permian deposits. However, at Burton a more local deviation in stresses seems to be taking place, which could be caused by the fold/fracture fabric of the local Carboniferous limestones. Joint and bedding directions have been measured on the outcrops adjacent to the site. The rose diagram given in Fig. 13 shows the presence of a dominant joint set striking approximately N–S, which has an average dip of 88° to the west, and a subordinate set striking approximately E–W having an average dip of 85° to the south. The sketch map given in Fig. 10 shows the average bedding plane dip directions and values, clearly defining a shallow syncline plunging gently to the south. The general coincidence of the trend of the fold axis and that of the main fracture set with the orientation of the measured contemporary stress direction (approximately N–S) suggests a local structural control.

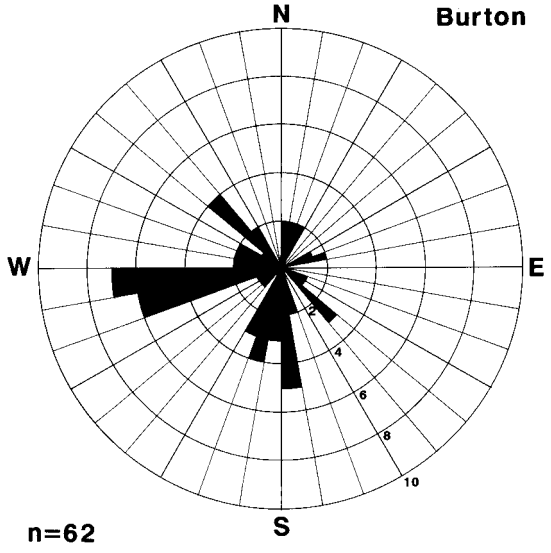

Fig. 13. Rose diagram showing the frequency of joints in terms of dip direction measured on the Crags in the vicinity of the Burton test site (see Fig. 10).

Stress magnitudes calculated from strain values are not only depth dependent, but also depend strongly on the mode of determination of elastic parameters. This raises the 'scale problem' in the selection of values for elastic parameters such as the Young's modulus. Although both uniaxial loading tests and larger-scale in situ Goodman Jack tests have been used for the determination of elastic parameters, the calculated stress magnitudes are still too high and therefore are considered to be only an indication of the upper stress magnitude limits at these test sites.

In general, shallow in situ stress data are not easy to interpret. However, the results reported here demonstrate that the methods employed in these field and laboratory studies, whilst not new in themselves, together offer effective approaches to obtaining reliable contemporary stress information. More specifically, principal stress orientation data can be recovered from shallow boreholes and rock cores when appropriate sites are selected.

Acknowledgements

Without the support of the Universities of Karlsruhe, Bristol and East Anglia, and also the British Geological Survey, these studies would not have been possible. We gratefully acknowledge the help and friendship of colleagues at these and other institutions over the years, particularly Paul Hancock, to whom this paper is dedicated. We thank the referees and editor for their reviews and C.G. Evans for his constructive comments. Institut für Geophysik, ETH Zürich, contribution no. 1130.

References

Amadei, B., 1983. Rock Anisotropy and the Theory of Stress Measurements. Springer, Berlin.

Becker, A., Paladini, S., 1990. In situ-Spannungen in Nord- und Mitteleuropa. Schr. Angew. Geol. Karlsruhe 10.

Becker, A., Paladini, S., 1992. Intra-plate stresses in Europe and plate-driving mechanisms. Ann. Tectonicae 6 (2), 173–192.

Becker, A., Werner, D., 1995. Neotectonic state of stress in the Jura Mountains. Geodinamica Acta 8 (2), 99–111.

Becker, A., Blenkinsop, T.G., Hancock, P.L., 1990. Comparison and tectonic interpretation of in situ stress measurements by flatjack and doorstopper techniques in Gloucestershire, England. Ann. Tectonicae 4 (1), 3–18.

Becker, A., Werner, D., Hancock, P.L., 1997. Theoretical considerations about residual strains around a magmatic dyke with application to the Castletown dyke, Scotland. N. Jb. Geol. Paläont. Abh. 203 (1), 77–88.

Brereton, N.R., Müller, B., 1991. European stress: contributions from borehole breakouts. Phil. Trans. R. Soc. Lond. A 337, 165–179.

Brereton, N.R., Chroston, P.N., Evans, C.J., Hudson, J.A., Whitmarsh, R.B., 1990. Stress in the oceanic crust: anelastic strain recovery and elastic properties of basaltic rocks. British Geological Survey Technical Report WK/90/10.

British Geological Survey, 1985. Thurso: Scotland Sheet 116(W), Solid Edition, scale 1:50,000.

Butterworth, S.R., 1993. Anelastic strain recovery of rock core and crustal stress measurements. Unpublished Ph.D. thesis, University of East Anglia.

Butterworth, S.R., Chroston, P.N., Davenport, C.A., Brereton, N.R., Evans, C.J., 1991. Anelastic strain recovery of rock core from the English Midlands. In: Roegiers, J.-C. (Ed.), Proceedings of the 32nd U.S. Symposium on Rock Mechanics. Balkema, Rotterdam, pp. 55–72.

Davenport, C.A., Ringrose, P.S., Becker, A., Hancock, P., Fenton, C., 1989. Geological investigations of late and post glacial earthquake activity in Scotland. In: Gregersen, S., Basham, P.W. (Eds.), Earthquakes at North-Atlantic Passive Margins: Neotectonics and Postglacial Rebound. Kluwer, Dordrecht, pp. 175–194.

Francis, E.H., Forsyth, I.H., Read, W.A., Armstrong, M., 1970. The Geology of the Stirling District. Mem. Geol. Surv. Great Britain. HMSO, Edinburgh.

Heuze, F.E., Amadei, B., 1985. The NX-borehole jack: a lesson in trials and errors. Int. J. Rock Mech. Min. Sci. Geomech. Abstr. 22 (2), 105–112.

Hiramatsu, Y., Oka, Y., 1962. Stress around a shaft or level excavated in ground with a three-dimensional stress state. Mem. Fac. Engng Kyoto Univ. 24, 56–76.

Jaeger, J.C., Cook, N.G.W., 1979. Fundamentals of Rock Mechanics. Chapman & Hall, London.

Leeman, E.R., 1964. Borehole rock stress measuring instruments, part 2. J. S. Afr. Inst. Min. Metall. 65, 82–114.

Leeman, E.R., 1971. The CSIR "doorstopper" and triaxial rock stress measuring instruments. Rock Mech. 3, 25–50.

Leeman, E.R., Hayes, D.J., 1966. A technique for determining the complete state of stress in rock using a single borehole. Proc. 1st Congr. Int. Soc. Rock Mech., Lisboa, Part II, pp. 17–23.

Lekhnitskii, S.G., 1963. Theory of Elasticity of an Anisotropic Elastic Body. Holden-Day, San Francisco.

Müller, B., Wehrle, V., Zeyen, H., Fuchs, K., 1997. Short-scale variations of tectonic stress regimes in the western European stress province north of the Alps and Pyrenees. Tectonophysics 275, 199–219.

Sissons, J.B., 1972. Dislocation and non-uniform uplift of raised shorelines in the western part of the Forth valley. Trans Inst. British Geogr. 55, 145–159.

Sissons, J.B., 1979. Palaeoclimatic inferences from former glaciers in Scotland and the Lake District. Nature 278, 518–521.

Whitmarsh, R.B., Bott, M.H.P., Fairhead, J.D., Kusznir, N.J., 1991. Tectonic stress in the lithosphere. Phil. Trans. R. Soc. Lond. A 337 (no. 1645).